PREDICTION MODEL OF INTERNAL HEAT GENERATION DURING WOOD BIOMASS DEGRADATION

Pedro Paulo O. Rodrigues [a], Giulia Cruz Lamas [a], Luiz Gustavo Galvão [b], Mayara Gabi Moreira [a], Thiago da Silva Gonzales [a], Patrick Rousset [c], Edgar A. Silveira [a]

a. University of Brasília, Mechanical Sciences Graduate Program, Laboratory of Energy and Environment, Brasilia-DF, 70910-900, Brazil.

b. Forest Products Laboratory (LPF), Brazilian Forest Service (SFB), Brasilia DF, 70818-900, Brazil

c. French Agriculture Research Centre for International Development (CIRAD), 73 Rue J. F. Breton, 34398, Montpellier, Cedex 5, France

ABSTRACT: Torrefaction is a thermochemical process where the biomass is subjected to temperatures between 200 and 300 °C in an inert or partially oxidative atmosphere to promote an energetic upgrade, adding value to this biofuel. Heat and mass transfer analysis is a complex transient problem that evolves an anisotropic medium with heterogeneous thermophysical properties during torrefaction. In addition, the processes advance with a complex set of degradation kinetics, developing endothermic and exothermic reactions that must be understood. Therefore, the present work aims to build a numerical model to analyze the thermodegradation kinetics and determine the heat generation within the biomass. The numerical modeling was established for *Eucalyptus grandis* biomass. First, a 0D kinetic model was built to predict the mass loss dynamics at one point (0D), applying a consecutive two-step reactions approximation discretized by the evolution of five pseudo-components. Second, an analysis of heat generation was established considering the solid degradation and organic groups that contemplate the released gases and their specific enthalpy. Finally, the processes were simulated considering the entire temperature range of torrefaction 200–300 °C for a 60 min treatment. The degradation prediction provided excellent goodness of fit with an R^2>0.99 for all treatments. The calculated enthalpy of solid and volatile pseudo components formation presented reliable correlations (R^2 > 0.99), providing the internal energy generation rate. The internal generation rates peaked between 20–40 min of treatment, the region where the biomass volatilization rate is maximum. The generation varied between approximately 25–400 W kg^{-1} of biomass, considering torrefaction treatment between 200–300 °C.

Keywords: Biomass; Torrefaction; Eucalyptus; Heat; Modeling

1 INTRODUCTION

The challenges of ensuring energy and environmental security arise from the interconnectedness of global development and the escalating anthropogenic emissions resulting from economic expansion [1]. In response to these concerns, Sustainable Development Goal 7 emphasizes prioritizing clean technology [2].

Biomass as a renewable resource has garnered significant interest as a suitable feedstock for various thermochemical processes, including combustion, gasification, and pyrolysis [3–7]. However, raw biomass exhibits several undesirable characteristics, such as low bulk energy density, high moisture content, rapid moisture uptake, and a substantial energy penalty for size reduction [8]. Therefore, torrefaction has emerged as a promising thermal pre-treatment technique to improve biomass's overall properties to solve these challenges [9–13]. In addition, the treatment adds more excellent commercial value to biomass, creating a more competitive scenario among the fuels available on the market.

Due to the time and temperature ranges of the process (200–300 °C) and low CO_2 emission, torrefaction presents a high potential to be used as upgrading pre-treatment within the production chain of this fuel [10,13]. However, due to the nature of the procedure, the treatment requires energy expenditure and adds costs to the material produced. Therefore, prediction models for evaluating the thermo-physical properties of biomass during treatment are of utmost importance for optimizing the process and minimizing energy expenditure and the production cost of treated biomass toward continuous reactors designed for industrial-scale operation.

Torrefaction treatment encompasses various physical and chemical phenomena within the biomass particles, such as convection, diffusion of volatile compounds, and external and internal heat transfer [14].

In the case of sufficiently small particles (2 mm), torrefaction generally does not encounter restrictions regarding heat and mass transfer [6,7]. Nevertheless, for industrial-scale torrefaction, preference is given to larger particles (>2 mm) to mitigate the high energy demand associated with grinding raw biomass [15–17]. In this scenario, significantly more intricate interactions occur where heat transfer restrictions lead to a temperature gradient within the particle, resulting in uneven chemical processes. In addition, the non-uniform heat release from exothermic decomposition reactions further enhances the process heterogeneity and may potentially trigger a thermal runaway [14,18].

Previous research has been conducted on torrefaction modeling of wood particle scale [8,13,19,20] and main wood components [21]. The studies focused on the two-step mechanism for kinetics description, pseudo-component evolution throughout torrefaction, and solid and volatile components description. However, only a few numerical studies assessed the set of degradation reactions and evaluated the behavior of the thermophysical properties of the biomass along the thermodegradation process through the torrefaction route [14,22,23]. Therefore, deep mechanisms discussion and insights concerning the heat generation prediction within biomass during torrefaction are still scarce in the literature.

In this context, the present work aims to build a Python script to analyze the thermodegradation kinetics and formulate equations to predict the solid yield, ultima composition of torrefied biomass, the composition of released volatiles and the heat generation within the biomass.

2 MATERIAL AND METHODS

2.1 Feedstock

Micro samples of a *Eucalyptus grandis* tree, investigated in the previous study [8,11,24], served as feedstock for the present study. The samples were harvested at the University of Brasilia's site for lignocellulosic biomass-controlled crops. The unprocessed material was crushed, sieved through a 60 mesh (0.250 mm) screen, and dried at 105 °C. Table I present the feedstock properties.

Table I. Proximate and elemental analyses of *Eucalyptus grandis* [8,11].

Raw material [8,11]	*Eucalyptus Grandis*
Proximate analysis (%) [a]	
Fixed carbon	19.02
Volatile matter	80.9
Ash	0.08
Ultimate analysis (%) [a]	
C	44.28
H	5.65
N	0.22
O [b]	49.85
Chemical formula	$CH_{1.53}\ O_{0.85}N_{0.004}$
Calorific (MJ kg^{-1})	
HHV	18.08

[a] Dry basis, [b] O calculated by difference.

2.2 TGA apparatus and torrefaction procedure

Torrefaction experiments were performed for 15mg samples using an SDT Q600 TGA from TA Instruments (relative error was controlled below 3%) [24]. The experimental apparatus contemplates a nitrogen steel cylinder, a rotameter (N_2 flow of 50 mL min^{-1}), a reaction unit (SDT Q600), and a torrefaction process control and data acquisition computer [24].

Torrefaction was performed at five temperatures (210, 230, 250, 270 and 290 °C, with a holding time of 60 min and a linear heating rate of 5 °C min^{-1} [24]. Before torrefaction, the samples were heated from room temperature to 105°C and maintained isothermally for 20min to ensure dry conditions [24].

The evaluation of thermal degradation behavior throughout torrefaction was conducted by comparing the dried weight prior to torrefaction (w_0) and the weight during torrefaction ($w_{i_{(t)}}$). The solid yield (S_Y) over time was determined with Eq. (1) [17,25–27], providing the instantaneous mass variation (TGA).

$$SY_{(t)} = \frac{w_{i_{(t)}}}{w_0} \times 100 \quad (1)$$

2.3 Kinetic modeling

The two-step kinetic model, firstly proposed by [28] and further optimized by [8,17,29], was applied to obtain kinetic reaction rates (solid (k_B, k_C) and volatile (k_{V1}, k_{V2})) and to predict the thermal degradation behavior. The model, uses a first-order mechanism composed by a two-step consecutive reactions (Eqs. (1) and (2)) and four reaction rates constants k_i (min-1, $i = B, C, V_1, V_2$) defined by the Arrhenius law [16].

$$1^{st}\text{ reaction step: } \begin{cases} A \xrightarrow{k_1} B \\ A \xrightarrow{k_{V_1}} V_1 \end{cases} \quad (2)$$

$$2^{nd}\text{ reaction step: } \begin{cases} B \xrightarrow{k_2} C \\ B \xrightarrow{k_{V_2}} V_2 \end{cases} \quad (3)$$

In this approach, the torrefaction products are lumped into five pseudo-components: solid (feedstock A, intermediate solid B and residue C) and volatiles V_1 and V_2 [28]. The total volatile is described by the sum of V_1 and V_2. Meanqhile, the total solid yield is expressed by the sum of masses of A, B, and C [28]. The model was applied by fitting numerical profiles to the experimental solid yield $S_Y^{(T)}(t)$ (obtained with TG equipment) using a fmincon minimization function in Matlab® [16]. Detailed model can be accessed in previous publications [8,15–17,27,30–33].

2.4 Prediction of the solid composition

The elemental composition of the solid pseudo-components was defined as a function of the relative reaction rates and the elemental composition of the raw material [19]. As a simplifying hypothesis, it is assumed that the elementary composition of the pseudo-component A is constant and equal to the composition of the material *in natura*. The composition of B and C defined based on the relative reaction rates and the elemental composition of the volatiles V_1 and V_2.

2.5 Prediction of the volatile composition

The model of the elemental composition of the volatile pseudo-components was defined according to the chemical species volatilized during the torrefaction process. Water, acetic acid, formic acid, methanol, lactic acid, furfural, hydroxyacetone, carbon dioxide, and carbon monoxide are the main chemicals volatilized in this process [34]. Water is the most abundant condensable chemical species among the non-condensable species, CO_2 is the dominant chemical volatiles [34].

These two hypotheses were used as a relationship between the proportions of volatilized chemical species, as shown in Eqs. (4–6), where the subscripts a to i denote acetic acid, water, formic acid, methanol, lactic acid, furfural, hydroxyacetone, carbon dioxide, and carbon monoxide, respectively.

$$Y_h < Y_b \quad (4)$$

$$Y_a, Y_c, Y_d, Y_e, Y_f, Y_g < Y_b \quad (5)$$

$$Y_h < Y_i \quad (6)$$

Disregarding nitrogen mass fraction in volatile compounds and assuming the elemental composition of the volatilized pseudo-components is constant throughout the treatment, the mass balance of carbon, hydrogen and oxygen was defined in Eq. (7), where Y_{C_j}, Y_{H_j}, Y_{O_j}, corresponding to the mass of carbon, hydrogen and oxygen, normalized by the molar mass of the chemical species n [8,19].

The term Y_{esp_n} corresponds to the mass of the species n, normalized by the total volatilized mass. The terms Y_{C_0}, Y_{H_0} and Y_{O_0} define the mass of carbon, hydrogen and oxygen in the raw biomass, the term Y_s corresponds to the resulting solid mass at the end of treatment, normalized by

the initial mass, obtained by simulating mass loss. $Y_{C_{tor}}$, $Y_{H_{tor}}$ and $Y_{O_{torrefied}}$ correspond to the normalized mass of carbon, hydrogen and oxygen obtained from the elemental analysis [8].

$$\begin{bmatrix} Y_{C_a} & \dots & Y_{C_a} \\ Y_{H_a} & \dots & Y_{H_a} \\ Y_{O_a} & \dots & Y_{O_a} \end{bmatrix} \begin{bmatrix} Y_a \\ \vdots \\ Y_i \end{bmatrix} = \begin{bmatrix} Y_{C_0} - Y_S Y_{C_{tor}} \\ Y_{H_0} - Y_S Y_{H_{tor}} \\ Y_{O_0} - Y_S Y_{O_{tor}} \end{bmatrix} \quad (7)$$

The solution for Eq. (7) was obtained by the function *linprog* from the *SciPy* library, supplemented in Python, applying the restriction conditions established in Eqs. (4–6). With the solution of Eq. (7), a new mass balance of the volatilized material was defined by Eq. (8) [19].

$$\begin{bmatrix} Y_{V_1}^{210} & Y_{V_2}^{210} \\ \vdots & \vdots \\ Y_{V_1}^{290} & Y_{V_2}^{290} \end{bmatrix} \begin{bmatrix} Y_{a,V_1} & \dots & Y_{i,V_1} \\ Y_{a,V_2} & \dots & Y_{i,V_2} \end{bmatrix} = \begin{bmatrix} Y_a^{210} & \dots & Y_i^{210} \\ \vdots & \dots & \vdots \\ Y_a^{290} & \dots & Y_i^{290} \end{bmatrix} \quad (8)$$

The system presented in Eq. (8) was solved using the least squares method, and the obtained result defines the proportion of chemical species present in the pseudo-components V_1 and V_2 and, therefore, their elementary compositions.

2.6 Prediction of the enthalpy of the reaction

The enthalpy of the formation of solid fuels can be approximated by their higher calorific value [22]. An approximation of enthalpy is presented in Eq. (9), where $H\widehat{HV}$, v_j and $\widehat{H_j^\circ}$ are the higher calorific value in J mol^{-1}, the number of moles of the product or reactant j (mol) and the enthalpy of formation of the products or reactants j in J mol^{-1}, respectively [35].

$$HHV \approx \sum_{j(reagents)} v_j \widehat{H_j^\circ} - \sum_{j(products)} v_j \widehat{H_j^\circ} \quad (9)$$

Complete combustion can be defined as a reaction Eq. (10), where the coefficients x and y represent the number of carbon and hydrogen atoms, respectively [36]. With the number of moles defined, the enthalpy of the formation of solid pseudo-components can be estimated based on their elemental composition, as in Eq. (11).

$$C_x H_y O_2 + \left(\frac{y + 4x - 4}{4}\right) O_2 \rightarrow \frac{y}{2} H_2O + xCO_2 \quad (10)$$

$$\widehat{H^\circ_{C_xH_yO_2}} \approx H\widehat{HV} + \frac{y}{2}\widehat{H^\circ_{H_2O}} + x\widehat{H_{CO_2}} \quad (11)$$

The HHV can be described as a function of the elemental composition of the biomass, as defined in Eq. (12) in J kg^{-1} [37].

$$HHV = 10^6 \times [(0.3328 Y_C) + (1.1576 Y_H) - (0.0608 Y_O) - 0.6875] \quad (12)$$

Therefore, the HHV can be defined for the solid pseudo-components A, B and C, relating the ultimate compositions of these pseudo-components.

The conversion step from $\widehat{H^\circ_{C_xH_yO_2}}$ in J mol^{-1} to $H^\circ_{C_xH_yO_2}$ in J kg^{-1} was established by dividing Eq. (11) and the molar mass of the solid biomass. Thus, Eq. (13) was obtained and the enthalpy of the reaction of the solid pseudo-components.

$$H^\circ_{C_xH_yO_2} \approx HHV + \frac{1}{x \cdot M_{M_C} + y \cdot M_{M_H} + 2 \cdot M_{M_O}} \left(\frac{y}{2}\widehat{H^\circ_{H_2O}} + x\widehat{H_{CO_2}}\right) \quad (13)$$

2.7 Prediction of the heat release (internal energy)

Two reaction steps were defined to estimate the energy released during the torrefaction process, converted into heat. In the first, the A pseudo-component is decomposed and in the second, B [22]. The enthalpy balances for the two decomposition reactions are described in Eqs. (11), and (12), where β, υ, γ and ξ are the relative reaction rates, and H_X° are the enthalpies of reaction of the pseudocomponents $X = (A, B, C, V_1, V_2)$.

$$\begin{cases} \Delta H_{r,1}^\circ = \beta H_B^\circ + \upsilon H_{V_1}^\circ - H_A^\circ \\ \beta = \dfrac{\mathcal{K}_1}{\mathcal{K}_1 + \mathcal{K}_{V_1}} \\ \upsilon = \dfrac{\mathcal{K}_{V_1}}{\mathcal{K}_1 + \mathcal{K}_{V_1}} \end{cases} \quad (14)$$

$$\begin{cases} \Delta H_{r,2}^\circ = \gamma H_C^\circ + \xi H_{V_2}^\circ - H_B^\circ \\ \gamma = \dfrac{\mathcal{K}_2}{\mathcal{K}_2 + \mathcal{K}_{V_2}} \\ \xi = \dfrac{\mathcal{K}_{V_2}}{\mathcal{K}_2 + \mathcal{K}_{V_2}} \end{cases} \quad (15)$$

The decomposition rates were defined in terms of the normalized masses Y_A and Y_B, of A and B by Eqs. (14) and (15), respectively [19]. The author also defined the rate of energy released $\dot{q}$ as the sum of the products of r_i and $\Delta H_{r,i}^\circ$, where i is the reaction step , as shown in Eq. (16).

$$\begin{aligned} -r_1 &= (k_1 + k_{V_1}) Y_A \\ -r_2 &= (k_2 + k_{V_2}) Y_B \\ \dot{q} &= -r_1 \Delta H_{r,1}^\circ - r_2 \Delta H_{r,2}^\circ \end{aligned} \quad (16)$$

3 RESULTS

3.1 Torrefaction

Figure 1 presents the thermodegradation prediction and the experimental data [8] for the five torrefaction temperatures (210, 230, 250, 270, and 290 °C).

As shown in Fig. 1, the results obtained in the mass loss simulations are suitable for fitting the experimental values observed in [8], which corroborates the validation of the observed results. Furthermore, as can be seen, the correlation points between the data are close to the perfect correlation curves for the five mass loss simulations, with an R^2 factor of 0.99 for all torrefaction conditions, in both mass loss curves (Fig. 1a) and their derivatives (Fig. 1b). Figure 2 presents the elemental composition and proportion of chemical species in volatile material.

As depicted in Fig. 2a, in volatile pseudo-component V_1, water and carbon dioxide constitute over 50% of its mass proportion. Previous studies [8] have indicated that in the initial stage of the computer simulation, the primary devolatilization mechanism is the formation of V_1. By considering the findings presented in Fig. 2a, it is evident that the formation of V_1 primarily drives the devolatilization of water at the process's inception, outweighing V_2 as a carbon fixation mechanism in the initial process. The results obtained indicate a more equitable distribution between the other volatilized components present in V_1 and V_2.

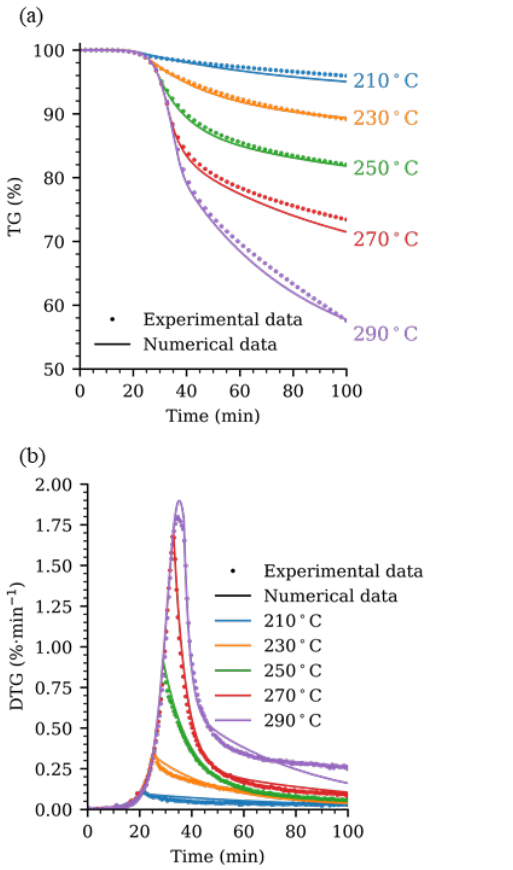

Figure 1: (a) Experimental data (TG profiles) from [8] and predicted data. (b) Derivative thermogravimetric (DTG) profiles and numerical prediction results.

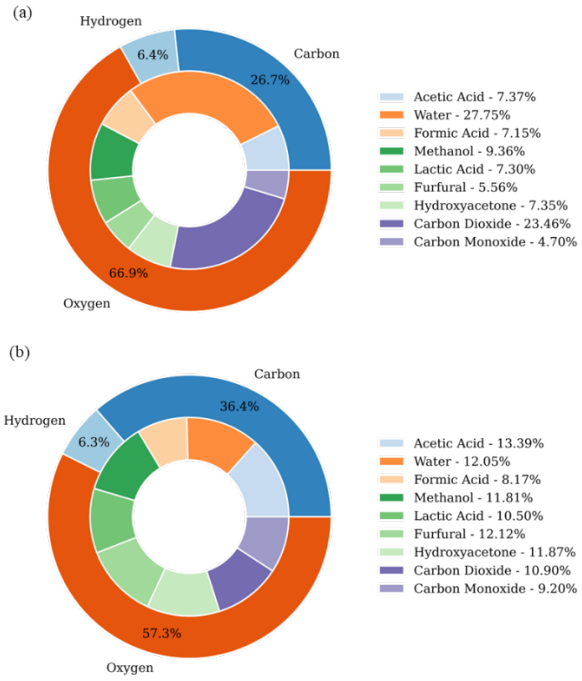

Figure 2: Elemental composition and proportion of chemical species in volatile material. (a) Volatile pseudocomponent V_1, (b) Volatile pseudocomponent V_2.

Fig. 3 depicts the prediction model results for heat generation during the torrefaction process, showing a continuous exothermic behavior and an increasing energy release rate with temperature. The heat release peaks range from 25.4 W kg^{-1} at 210 °C treatment to 432.1 W kg^{-1} at 290 °C. A similarity is evident between the numerical curves of mass loss (Fig. 1b) and released energy (Fig. 3), as observed by comparing the two figures. Mass loss and energy release peaks coincide in terms of timing. This similarity suggests that the released heat is more closely associated with the overall mass loss process (volatile formation and release) than a specific pseudo-component's mass loss.

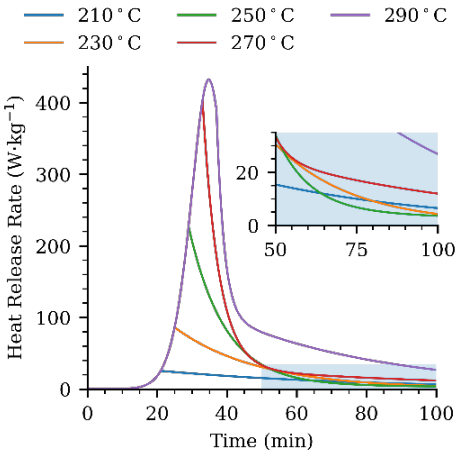

Figure 3: Heat release rate normalized by initial mass of torrefied material.

4 CONCLUSIONS AND FUTURE DIRECTIONS

In this work, a thermochemical degradation kinetics model was developed and validated with a high R^2 value of 0.99. This model allowed for the evaluation of the elemental composition of biomass during torrefaction, enabling more accurate projections of energy gains in wood subjected to this treatment. The thermophysical properties of biomass were modeled using established and validated models from the literature, allowing for the assessment of specific mass, reaction enthalpies, energy release, thermal conductivity, and specific heat at a constant pressure throughout the torrefaction process. The simulation data was validated against literature data for other species.

The proposed mathematical model and constraint conditions for volatile material prediction provided results closely aligned with the literature. Furthermore, this contribution enables the determination of chemical proportions in volatilized pseudo-components based on the specific elemental composition of each torrefied biomass. Therefore, enhancing the accuracy of energy release predictions during the torrefaction process.

5 REFERENCES

[1] A.E. Torkayesh, B. Malmir, M. Rajabi Asadabadi, Sustainable waste disposal technology selection: The stratified best-worst multi-criteria decision-making method, Waste Manag. 122 (2021) 100–112. https://doi.org/10.1016/j.wasman.2020.12.040.

[2] United Nations, The Sustainable Development Goals Report 2021, United Nations, 2021. https://doi.org/10.18356/9789210056083.

[3] G.C. Lamas, B. S. Chaves, P.P. Oliveira, T. Barbosa, T. da S. Gonzales, G.F. Ghesti, P. Rousset, E.A. Silveira, Effect of torrefaction on steam-enhanced co-gasification of an urban forest and landfill waste blend: H2 production and CO2 emissions mitigation, Int. J. Hydrogen Energy. (2023). https://doi.org/https://doi.org/10.1016/j.ijhydene.2023.03.367.

[4] E.A. Silveira, B. Santanna Chaves, L. Macedo, G.F. Ghesti, R.B.W. Evaristo, G. Cruz Lamas, S.M. Luz, T. de P. Protásio, P. Rousset, A hybrid optimization approach towards energy recovery from torrefied waste blends, Renew. Energy. (2023). https://doi.org/10.1016/j.renene.2023.05.053.

[5] J.P. Rodrigues, G.F. Ghesti, E.A. Silveira, G.C. Lamas, R. Ferreira, M. Costa, Waste-to-hydrogen via CO2/Steam-enhanced gasification of spent coffee ground, Clean. Chem. Eng. 4 (2022) 100082. https://doi.org/10.1016/j.clce.2022.100082.

[6] G.F. Ghesti, E.A. Silveira, M.G. Guimarães, R.B.W.W. Evaristo, M. Costa, Towards a sustainable waste-to-energy pathway to pequi biomass residues: Biochar, syngas, and biodiesel analysis, Waste Manag. 143 (2022) 144–156. https://doi.org/10.1016/j.wasman.2022.02.022.

[7] R.B.W. Evaristo, R. Ferreira, J. Petrocchi Rodrigues, J. Sabino Rodrigues, G.F. Ghesti, E.A. Silveira, M. Costa, Multiparameter-analysis of CO2/Steam-enhanced gasification and pyrolysis for syngas and biochar production from low-cost feedstock, Energy Convers. Manag. X. 12 (2021) 100138. https://doi.org/10.1016/j.ecmx.2021.100138.

[8] E.A. Silveira, S.M. Luz, R.M. Leão, P. Rousset, A. Caldeira-Pires, Numerical modeling and experimental assessment of sustainable woody biomass torrefaction via coupled TG-FTIR, Biomass and Bioenergy. 146 (2021) 105981. https://doi.org/10.1016/j.biombioe.2021.105981.

[9] S.K. Thengane, K.S. Kung, A. Gomez-Barea, A.F. Ghoniem, Advances in biomass torrefaction: Parameters, models, reactors, applications, deployment, and market, Prog. Energy Combust. Sci. 93 (2022) 101040. https://doi.org/10.1016/j.pecs.2022.101040.

[10] E.A. Silveira, L.A. Macedo, K. Candelier, P. Rousset, J.-M. Commandré, Assessment of catalytic torrefaction promoted by biomass potassium impregnation through performance indexes, Fuel. 304 (2021) 121353. https://doi.org/10.1016/j.fuel.2021.121353.

[11] E.A. Silveira, S. Luz, K. Candelier, L.A. Macedo, P. Rousset, An assessment of biomass torrefaction severity indexes, Fuel. 288 (2021) 119631. https://doi.org/10.1016/j.fuel.2020.119631.

[12] L.A. Macedo, E.A. Silveira, P. Rousset, J. Valette, J.-M. Commandré, Synergistic effect of biomass potassium content and oxidative atmosphere: Impact on torrefaction severity and released condensables, Energy. 254 (2022) 124472. https://doi.org/10.1016/j.energy.2022.124472.

[13] E.A. Silveira, L.A. Macedo, P. Rousset, K. Candelier, L.G.O. Galvão, B.S. Chaves, J.-M. Commandré, A potassium responsive numerical path to model catalytic torrefaction kinetics, Energy. 239 (2022) 122208. https://doi.org/10.1016/j.energy.2021.122208.

[14] R.B. Bates, A.F. Ghoniem, Modeling kinetics-transport interactions during biomass torrefaction: The effects of temperature, particle size, and moisture content, Fuel. 137 (2014) 216–229. https://doi.org/10.1016/j.fuel.2014.07.047.

[15] E.A. Silveira, M.S. Santanna, N.P. Barbosa Souto, G.C. Lamas, L.G.O. Galvão, S.M. Luz, A. Caldeira-Pires, Urban lignocellulosic waste as biofuel: thermal improvement and torrefaction kinetics, J. Therm. Anal. Calorim. 148 (2023) 197–212. https://doi.org/10.1007/s10973-022-11515-0.

[16] E.A. Silveira, B.J. Lin, B. Colin, M. Chaouch, A. Pétrissans, P. Rousset, W.H. Chen, M. Pétrissans, Heat treatment kinetics using three-stage approach for sustainable wood material production, Ind. Crops Prod. 124 (2018) 563–571. https://doi.org/10.1016/j.indcrop.2018.07.045.

[17] B.-J. Lin, E.A. Silveira, B. Colin, W.-H. Chen, Y.-Y. Lin, F. Leconte, A. Pétrissans, P. Rousset, M. Pétrissans, Modeling and prediction of devolatilization and elemental composition of wood during mild pyrolysis in a pilot-scale reactor, Ind. Crops Prod. 131 (2019) 357–370. https://doi.org/10.1016/j.indcrop.2019.01.065.

[18] P. Perré, R. Rémond, I. Turner, A comprehensive dual-scale wood torrefaction model: Application to the analysis of thermal run-away in industrial heat treatment processes, Int. J. Heat Mass Transf. 64 (2013) 838–849. https://doi.org/10.1016/j.ijheatmasstransfer.2013.03.066.

[19] R.B. Bates, A.F. Ghoniem, Biomass torrefaction: Modeling of volatile and solid product evolution kinetics, Bioresour. Technol. 124 (2012) 460–469. https://doi.org/10.1016/j.biortech.2012.07.018.

[20] M. Chai, L. Xie, X. Yu, X. Zhang, Y. Yang, M.M. Rahman, P.H. Blanco, R. Liu, A. V. Bridgwater, J. Cai, Poplar wood torrefaction: Kinetics, thermochemistry and implications, Renew. Sustain. Energy Rev. 143 (2021). https://doi.org/10.1016/j.rser.2021.110962.

[21] W.-H.H. Chen, C. Fong Eng, Y.-Y.Y. Lin, Q.-V.V. Bach, V. Ashokkumar, P.-L.L. Show, Two-step thermodegradation kinetics of cellulose, hemicelluloses, and lignin under isothermal torrefaction analyzed by particle swarm optimization, Energy Convers. Manag. 238 (2021) 114116. https://doi.org/10.1016/j.enconman.2021.114116

[22] R.B. Bates, A.F. Ghoniem, Biomass torrefaction: modeling of reaction thermochemistry., Bioresour. Technol. 134 (2013) 331–40. https://doi.org/10.1016/j.biortech.2013.01.158.

[23] Y. Haseli, Process Modeling of a Biomass Torrefaction Plant, Energy and Fuels. 32 (2018) 5611–5622. https://doi.org/10.1021/acs.energyfuels.7b03956.

[24] E.A. Silveira, S.M. Luz, R.M. Leão, P. Rousset, A. Caldeira-Pires, Numerical modeling and experimental assessment of sustainable woody biomass torrefaction via coupled TG-FTIR, Biomass and Bioenergy. 146 (2021). https://doi.org/10.1016/j.biombioe.2021.105981.

[25] E.A. Silveira, M.V.G. de Morais, P. Rousset, A.

Caldeira-Pires, A. Pétrissans, L.G.O. Galvão, Coupling of an acoustic emissions system to a laboratory torrefaction reactor, J. Anal. Appl. Pyrolysis. 129 (2018) 29–36. https://doi.org/10.1016/j.jaap.2017.12.008.

[26] E.A. Silveira, B. Lin, B. Colin, A. Pétrissans, P. Rousset, Mathematical approach to build a numerical tool for mass loss prediction during wood torrefaction, in: Veikko Möttönen and Emilia Heinonen (Ed.), 6th Int. Sci. Conf. Hardwood Process., Natural Resources Institute Finland (Luke), Helsinki, 2017: pp. 272–279. http://urn.fi/URN:ISBN:978-952-326-509-7.

[27] B. Lin, E.A. Silveira, B. Colin, M. Chaouch, A. Pétrissans, P. Rousset, M. Pétrissans, Experimental and numerical analysis of poplar thermodegradation, in: V.M. and E. Hein (Ed.), 6th Int. Sci. Conf. Hardwood Process., Natural Resources Institute Finland, Helsinki, 2017: pp. 319–325. http://urn.fi/URN:ISBN:978-952-326-509-7.

[28] C. Di Blasi, M. Lanzetta, Intrinsic kinetics of isothermal xylan degradation in inert atmosphere, J. Anal. Appl. Pyrolysis. 40–41 (1997) 287–303. https://doi.org/10.1016/S0165-2370(97)00028-4.

[29] E.A. Silveira, S. Luz, M.S. Santanna, R.M. Leão, P. Rousset, A.C.- Pires, Thermal upgrading of sustainable woody material: experimental and numerical torrefaction assessment, in: 28th Eur. Biomass Conf. Exhib., Virtual, 2020: pp. 694–698. https://doi.org/10.5071/28thEUBCE2020-3CV.2.5.

[30] E.A. Silveira, L.G. Oliveira Galvão, L. Alves de Macedo, I. A. Sá, B. S. Chaves, M.V. Girão de Morais, P. Rousset, A. Caldeira-Pires, Thermo-Acoustic Catalytic Effect on Oxidizing Woody Torrefaction, Processes. 8 (2020) 1361. https://doi.org/10.3390/pr8111361.

[31] L.G.O.B.S.C. Galvão, M.V.G. de Morais, A.T. do V. Vale, A. Caldeira-Pires, P. Rousset, E.A. Silveira, Combined thermo-acoustic upgrading of solid fuel: experimental and numerical investigation, 28th Eur. Biomass Conf. Exhib. (2020) 6–9. https://doi.org/10.5071/28thEUBCE2020-3DO.6.2.

[32] B.-J. Lin, E.A. Silveira, B. Colin, W.-H. Chen, A. Pétrissans, P. Rousset, M. Pétrissans, Prediction of higher heating values (HHVs) and energy yield during torrefaction via kinetics, Energy Procedia. 158 (2019) 111–116. https://doi.org/10.1016/j.egypro.2019.01.054.

[33] E.A. Silveira, L. Macedo, P. Rousset, J.-M. Commandré, L.G.O. Galvão, B.S. Chaves, The effect of potassium carbonate wood impregnation on torrefaction kinetics, in: 29th Eur. Biomass Conf. Exhib., 2021. https://doi.org/10.5071/29thEUBCE2021-3DV.6.4.

[34] M.J. Prins, K.J. Ptasinski, F.J.J.G. Janssen, Torrefaction of wood: Part 2. Analysis of products, J. Anal. Appl. Pyrolysis. 77 (2006) 35–40. https://doi.org/10.1016/j.jaap.2006.01.001.

[35] D. Merrick, Mathematical models of the thermal decomposition of coal: 2. Specific heats and heats of reaction, Fuel. 62 (1983) 540–546. https://doi.org/10.1016/0016-2361(83)90223-5.

[36] S. Erdoğan, LHV and HHV prediction model using regression analysis with the help of bond energies for biodiesel, Fuel. 301 (2021). https://doi.org/10.1016/J.FUEL.2021.121065.

[37] Optimal use of condensed parameters of ultimate analysis to predict the calorific value of biomass, Fuel. 214 (2018) 640–646. https://doi.org/10.1016/j.fuel.2017.10.082.

6 ACKNOWLEDGEMENTS

The research presented was supported by Brazilian National Council for Scientific and Technological Development (CNPq), DPI/UnB, Brazilian Forest Products Laboratory (LPF), and the Federal District Research Foundation (FAPDF – Fundação de Apoio à Pesquisa do Distrito Federal, Edital 3/2021 – Project 00193.00000756/2021-35) for the financial support.

6 LOGO SPACE